Enthalpies of formation of lanthanide oxyapatite phases

A.S. Risbud
Department of Applied Physics, California Institute of Technology, MC 128-95, Pasadena, California 91125

K.B. Helean
Thermochemistry Facility, Department of Chemical Engineering and Materials Science, University of California at Davis, Davis, California 95616

M.C. Wilding
Department of Geology, University of California at Davis, Davis, California 95616

P. Lu
Department of Physics, Harvard University, Cambridge, Massachusetts 02138

A. Navrotsky[a)]
Thermochemistry Facility, Department of Chemical Engineering and Materials Science, University of California at Davis, Davis, California 95616

(Received 13 June 2001; accepted 2 August 2001)

A family of lanthanide silicates adopts an oxyapatitelike structure with structural formula $Ln_{9.33}\square_{0.67}(SiO_4)_6O_2$ (Ln = La, Sm, Nd, Gd, $\square$ = vacancy). The enthalpies of solution, ΔH_S, for these materials and their corresponding binary oxides were determined by high-temperature oxide melt solution calorimetry using molten $2PbO \cdot B_2O_3$ at 1078 K. These data were used to complete thermodynamic cycles to calculate enthalpies of formation from the oxides, $\Delta H^0_{\text{f-oxides}}$ (kJ/mol): $La_{9.33}\square_{0.67}(SiO_4)_6O_2$ = −776.3 ± 17.9, $Nd_{9.33}\square_{0.67}(SiO_4)_6O_2$ = −760.4 ± 31.9, $Sm_{9.33}\square_{0.67}(SiO_4)_6O_2$ = −590.3 ± 18.6, and $Gd_{9.33}\square_{0.67}(SiO_4)_6O_2$ = −446.9 ± 21.9. Reference data were used to calculate the standard enthalpies of formation from the elements, ΔH^0_f (kJ/mol): $La_{9.33}\square_{0.67}(SiO_4)_6O_2$ = −14611.0 ± 19.4, $Nd_{9.33}\square_{0.67}(SiO_4)_6O_2$ = −14661.5 ± 32.2, $Sm_{9.33}\square_{0.67}(SiO_4)_6O_2$ = −14561.7 ± 20.8, and $Gd_{9.33}\square_{0.67}(SiO_4)_6O_2$ = −14402.7 ± 28.2. The formation enthalpies become more endothermic as the ionic radius of the lanthanide ion decreases.

Lanthanide oxyapatites, $Ln_{9.33}\square_{0.67}(SiO_4)_6O_2$ (Ln = La, Sm, Nd, Gd, $\square$ = vacancy), have many interesting applications. Lanthanides are used as sintering aids during silicon nitride synthesis resulting in Ln oxyapatite formation at grain triple junctions in silicon nitride ceramics.[1] In addition, there is increasing interest in Gd-containing compounds because of their high luminescence efficiency when doped with other rare-earth ions.[2–4] Many of these properties can be attributed to the unique oxyapatite structure that contains oxygen atoms located in the hexagonal tunnels parallel to the *c* axis. These oxygen atoms are bonded to Ln cations but are not bonded to Si and are therefore isolated from Si tetrahedra.[5] Ln oxyapatites are potentially useful for modeling the release of actinides from ceramic nuclear waste forms.[6,7] Thermodynamic measurements are critical in evaluating the phase stability of the Ln oxyapatites. The lack of experimental data motivated the present work on the correlation of enthalpies of formation to changes in the ionic radii of the lanthanide in the oxyapatite structure.

The Ln oxyapatite phases were synthesized using a solid-state sintering process. A mechanical mixture of Ln_2O_3 (Ln = La, Nd, Sm, Gd) and SiO_2-quartz according to the stoichiometric ratio $7Ln_2O_3$:$9SiO_2$ was prepared in a glove box under an argon atmosphere. This mixture was ground into a fine powder, pressed into a 3-g pellet, and was sintered in air in a platinum crucible for 180 h at 1500 °C to achieve the formation of the lanthanide silicate phase according to the reaction

$$14/3\ Ln_2O_3 + 6SiO_2 \rightarrow Ln_{9.33}\square_{0.67}(SiO_4)_6O_2 \quad . \quad (1)$$

The sintered samples were analyzed by powder x-ray diffraction (XRD) on a Scintag PAD-V diffractometer (Scintag, Inc. a division of Thermo, Cupertino, CA) using Cu K_α radiation, a beam voltage of 45 kV, and 0.02° step size from 18° to 90° 2θ with a 5-s dwell time.

[a)]Address all correspondence to this author.
e-mail: anavrotsky@ucdavis.edu

Powder XRD analysis of these samples indicated that the phase formed was oxyapatite ($P6_3/m$).[8] A least-squares refinement of the XRD data using Si as an internal standard was used to determine the lattice parameters (Table I).

An analysis of the XRD data indicated that, for Sm, Nd, and La oxyapatite, excess Ln_2O_3 was present in the samples. Using the relative intensity ratios of the peaks for each oxyapatite sample and its corresponding Ln_2O_3 impurity, the weight percent impurity was estimated. The Sm oxyapatite had approximately 7.9 wt% impurity, while the La and Nd oxyapatites had 4.0 and 1.6 wt% impurities, respectively. The Gd oxyapatite showed no impurity peaks in the XRD pattern. The finer particle size of the starting Gd_2O_3 powder compared to the other rare-earth oxides may have resulted in increased reactivity.

Electron microprobe analysis was used to assess sample homogeneity and to conduct quantitative wave dispersive spectroscopic (WDS) chemical analyses. A Cameca SX50 (Courbevoic, France) microprobe was used with an accelerating voltage of 20 kV and a spot size of 1 micron. Samples were analyzed against $LnPO_4$ and SiO_2 standards.

Backscattered electron (BSE) imaging indicated that the primary phase was Ln oxyapatite. No impurity phases were observed by BSE in the Gd oxyapatite sample. Significant impurities were observed in the Sm, Nd, and La phases. The observed impurities appeared on edges of grains and at pores in the loosely sintered ceramics. The small size of the impurity grains (≈2 microns thick) and their intergrowth with the oxyapatite phase made quantitative chemical analysis difficult. However, WDS analysis of several impurity grains indicated that the bulk (>98 wt%) of the material was Ln_2O_3. Digital analysis of BSE images indicated that the Nd oxyapatite contained approximately 1 vol% Nd_2O_3 impurity. Analysis of the BSE images for the Sm oxyapatite indicated that this sample contained approximately 5 vol% Sm_2O_3 impurity. The La oxyapatite sample contained approximately 5 vol% La_2O_3 impurity. This is in reasonable agreement with the results of the XRD analysis.

TABLE I. Lattice parameters for Ln oxyapatite phases determined by powder XRD least-squares analysis using Si as an internal standard.

$Ln_{9.33}\square_{0.67}(SiO_4)O_2$	Lattice parameter *a*, Å	Lattice parameter *c*, Å	Vol. (Å^3)
Gd	9.4453 (11)	6.8706 (6)	530.83
Sm	9.4920 (5)	6.9354 (4)	541.15
Nd	9.5723 (8)	7.0303 (7)	555.57
La	9.7246 (11)	7.1919 (6)	589.01
Reference data			
Nd[7]	9.5731 (8)	7.0336 (2)	···
La[7]	9.7259 (10)	7.1899 (3)	···

Errors are reported in parentheses. Reference values for Nd and La oxyapatite are reported for comparison.

Quantitative WDS analysis indicated that the Ln oxyapatite samples have, within error, their nominal stoichiometry (Table II). Even though these samples were sintered for 180 h at high temperature (1500 °C), they sintered poorly and consisted of loose grains of fine powder. This made precise quantitative chemical analysis difficult. The uneven surface of powder probe samples greatly increased the scatter in the data.[9] As a result, the normalized data were used to calculate the sample stoichiometry.

If the starting material was stoichiometric, then excess SiO_2 must be present in the ratio $7Ln_2O_3$:$9SiO_2$. Significant peak overlaps with the oxyapatite phase and SiO_2 preclude the quantitative determination of this impurity from XRD results. SiO_2 would not easily be observed in BSE images if it precipitated out along grain boundaries. To assess the impact of the uncertainty of the impurity content on the calorimetric data, two corrections were applied. The first assumed only Ln_2O_3 as an impurity and the second assumed that SiO_2 is also present in stoichometric proportions (Table III). The SiO_2 correction made no significant difference to the ΔH_{ds} values for Ln oxyapatite (Table IV).

High-temperature oxide melt solution calorimetry was used to measure the enthalpies of drop solution for the oxyapatite samples plus their binary oxide components (Table IV). A Calvet-type calorimeter with a twinned design was used to collect drop solution data. The calorimeter design and techniques are described in detail elsewhere.[10,11] Two types of experiments were conducted. Drop solution enthalpies, ΔH_{ds}, were measured by dropping pellets (≈5 mg) of the powder sample from room temperature into the lead borate solvent ($2PbO \cdot B_2O_3$) at calorimeter temperature (1078 K). Thus, these measurements consist of two components, the heat content of the sample, $\int_{298}^{1078} C_p dT$, and the heat of solution, ΔH_s. A second set of experiments was

TABLE II. WDS analyses of Ln oxyapatite phases.

$Ln_{9.33}\square_{0.67}(SiO_4)_6O_2$	Ln_2O_3 (wt%)	SiO_2 (wt%)	Total
Gd measured	82.76 (0.69)	16.57 (0.58)	99.33 (0.85)
Gd normalized	83.32 (0.52)	16.68 (0.52)	100.00
Gd theoretical	82.45	17.57	100.00
Sm measured	80.29 (1.60)	18.64 (0.71)	98.92 (2.25)
Sm normalized	81.17 (0.36)	18.83 (0.36)	100.00
Sm theoretical	81.89	18.14	100.00
Nd measured	80.40 (2.22)	18.71 (0.79)	99.11 (2.73)
Nd normalized	81.12 (0.57)	18.88 (0.57)	100.00
Nd theoretical	81.35	18.68	100.00
La measured	81.54 (3.78)	18.70 (0.55)	100.21 (3.76)
La normalized	81.54 (1.13)	18.46 (1.13)	100.00
La theoretical	80.85	19.17	100.00

Errors are calculated as one standard deviation of the mean and are reported in parentheses. Normalized and theoretical values are given for comparison.

TABLE III. Estimated impurity content of the Ln oxyapatite samples.

	$Ln_{9.33}\square_{0.67}(SiO_4)_6O_2$ (wt.%)	Ln_2O_3 (wt.%)	SiO_2 (wt.%)
Gd	100	…	…
Sm	81.7	8	10.3
Nd	95.3	2	2.7
La	88.6	5	6.4

The Ln_2O_3 impurities were estimated using XRD and BSE. The presumed SiO_2 impurity was estimated from stoichiometry.

conducted in the absence of solvent. These so-called transposed temperature drop experiments, ΔH_{ttd}, measure the heat content directly. Solution enthalpies, ΔH_s, are calculated by subtracting ΔH_{ttd} from ΔH_{ds}.

Enthalpies of solution, ΔH_s, were calculated for the Ln_2O_3 and SiO_2 samples so that these data could be compared to literature values (Table IV).[12,13] The ΔH_s values for Gd_2O_3, Sm_2O_3, and La_2O_3 are equal, within error, to the values previously reported. The ΔH_s value for Nd_2O_3 is more exothermic by 9.5 kJ/mol than the previously reported value. This discrepancy may be due to the small (−0.5 kJ/mol) measured ΔH_{ds} value for Nd_2O_3 in Pb borate at 1078 K. The drop solution experiments for Nd_2O_3 gave only very small heat effects and were consequently not considered reliable. Due to the experimental difficulties with measuring ΔH_{ds} (Nd_2O_3) and the excellent agreement between the calculated ΔH_s values for Gd_2O_3, Sm_2O_3, La_2O_3 and the previously published data, the literature data for ΔH_s (Nd_2O_3) was used to calculate a ΔH_{ds} (Nd_2O_3) value (Table IV).[13] The efficacy of this approach was verified by measuring ΔH_s (Nd_2O_3) directly, which gave a value of −87.6 ± 6.3 kJ/mol, which agrees with the previously published value. The ΔH_{ds} (Nd_2O_3) value was calculated by adding ΔH_s and ΔH_{ttd} which gives a value of 9.0 ± 5.8 kJ/mol. The ΔH_s value for quartz differed from the previously reported value by 1.5 kJ/mol,[12] which is comparable to the expected uncertainty due to impurities.

The formation enthalpies, $\Delta H^0_{\text{f-oxides}}$, of the Ln oxyapatites were derived from the ΔH_{ds} data (Table V). Errors are propagated in the thermodynamic cycle assuming linear combinations of independent variables. The calculated values for $\Delta H^0_{\text{f-oxides}}$ as well as $\Delta H^0_{\text{f-elements}}$ are reported (Table VI). Reference values for $\Delta H^0_{\text{f-elements}}$ for the binary oxide components were used to calculate the standard enthalpies of formation for the Ln oxyapatite phases.[14]

Three conclusions can be drawn from these data. First, the Ln oxyapatite phases studied are substantially stable with respect to their binary oxides. Second, the general trend in formation enthalpies as a function of ionic potential (Z/r) indicates that the Ln oxyapatite phase becomes increasingly more stable as the ionic potential decreases, i.e., as the ionic radius of the Ln ion becomes larger (Fig. 1). Conversely, decreasing the ionic radii beyond Gd destabilizes the oxyapatite phase with respect to enthalpy allowing for the possible formation of other Ln silicate structures. This observation is consistent with previous reports that Sm and Eu showed a strong tendency toward forming the oxyapatite structure whereas Ho and Er did not.[7] At Ln = Gd another Ln-silicate structure occurred along with the oxyapatite phase, $Ln_2Si_2O_7$ ($P2_1/c$).[7] This is an indication that these two phase assemblages are similar in energy. The third conclusion is that the stabilization effect of increasing ionic radii of the Ln-site ion is not a linear function. Substituting Nd for Sm stabilizes the Ln oxyapatite structure by 122 kJ/mol. Substituting La for Nd stabilizes the structure by 64 kJ/mol. Relatively little additional stabilization of the oxyapatite structure is gained by increasing the ionic radii of the lanthanide ion beyond Nd as shown

TABLE IV. Enthalpies of drop solution, ΔH_{ds}, for Ln oxyapatite, Ln_2O_3, and SiO_2 quartz and heat contents, ΔH_{ttd}, and solution enthalpies, ΔH_s, for Ln_2O_3 and SiO_2 quartz.

Compound	ΔH_{ds}(kJ/mol)	ΔH_{ttd}(kJ/mol)	ΔH_s(kJ/mol) calculated	ΔH_s(kJ/mol) Refs. 12,13[a]
Gd_2O_3	19.6 ± 1.8 (5)	93.4 ± 2.4 (4)	−73.8 ± 3.0	−72.6 ± 3.4
Sm_2O_3	21.8 ± 2.5 (8)	107.4 ± 3.0 (4)	−85.6 ± 3.9	−79.4 ± 4.2
Nd_2O_3	−0.5 ± 0.2 (2)	98.2 ± 1.6 (4)	−98.7 ± 1.6	−89.2 ± 5.6
La_2O_3	−27.8 ± 0.2 (3)	97.8 ± 1.0 (4)	−125.6 ± 1.0	−126.0 ± 4.4
SiO_2 quartz	49.8 ± 1.0 (11)	51.1 ± 0.9 (8)	−1.3 ± 1.3	−4.3 ± 0.2
		ΔH_{ds}(kJ/mol)[b]	ΔH_{ds}(kJ/mol)[c]	
$Gd_{9.33}\square_{0.67}(SiO_4)_6O_2$		837.2 ± 21.4 (10)	837.2 ± 21.4 (10)	
$Sm_{9.33}\square_{0.67}(SiO_4)_6O_2$		990.9 ± 17.7 (7)	989.9 ± 17.1 (7)	
$Nd_{9.33}\square_{0.67}(SiO_4)_6O_2$		1056.9 ± 31.8 (5)	1056.5 ± 31.8 (5)	
$La_{9.33}\square_{0.67}(SiO_4)_6O_2$		934.0 ± 17.7 (4)	933.2 ± 23.3 (4)	

The solvent was $2PbO \cdot B_2O_3$ at 1078 K. Errors are calculated as two standard deviations of the mean. Number of experiments is reported in parentheses. Reference values of ΔH_s for Ln_2O_3 and quartz are given for comparison.

[a]Data gathered at 975 K.

[b]Data corrected for excess Ln_2O_3.

[c]Data corrected for excess Ln_2O_3 and SiO_2.

TABLE V. The thermodynamic cycle used for the calculation of the enthalpies of formation from the oxides for Ln oxyapatite (Ln = Gd, Sm, Nd, La).

ΔH_{ds} (Ln_2O_3)	$Ln_2O_{3\ (crystal,298\ K)} \rightarrow Ln_2O_{3\ (sol,1078\ K)}$
ΔH_{ds} (SiO_2)	$SiO_{2\ (crystal,298\ K)} \rightarrow SiO_{2\ (sol,1078\ K)}$
ΔH_{ds} (Ln oxyapatite)	$Ln_{9.33}\square_{0.67}(SiO_4)_6O_{2\ (crystal,298\ K)} \rightarrow 14/3Ln_2O_{3(sol,1078\ K)} + 6SiO_{2(sol,1078\ K)}$
$\Delta H^0_{f\text{-oxides}}$	$= 14/3\Delta H_{ds}(Ln_2O_3) + 6\Delta H_{ds}(SiO_2) - \Delta H_{ds}$(Ln oxyapatite)

TABLE VI. The $\Delta H^0_{f\text{-oxides}}$ and the standard enthalpy of formation from the elements for Ln oxyapatite phases (kJ/mol).

Compound	$\Delta H^0_{f\text{-oxides}}$	$\Delta H^0_{f\text{-elements}}$
$Gd_{9.33}\square_{0.67}(SiO_4)_6O_2$	−446.9 ± 21.9	−14402.7 ± 28.2
$Sm_{9.33}\square_{0.67}(SiO_4)_6O_2$	−589.4 ± 23.2	−14561.7 ± 20.8
$Nd_{9.33}\square_{0.67}(SiO_4)_6O_2$	−715.7 ± 32.4	−14616.8 ± 32.2
$La_{9.33}\square_{0.67}(SiO_4)_6O_2$	−764.1 ± 23.4	−14599.6 ± 26.1

$\Delta H^0_{f\text{-elements}}$ calculated using reference data.[15] Errors are propagated assuming linear combinations of independent variables.

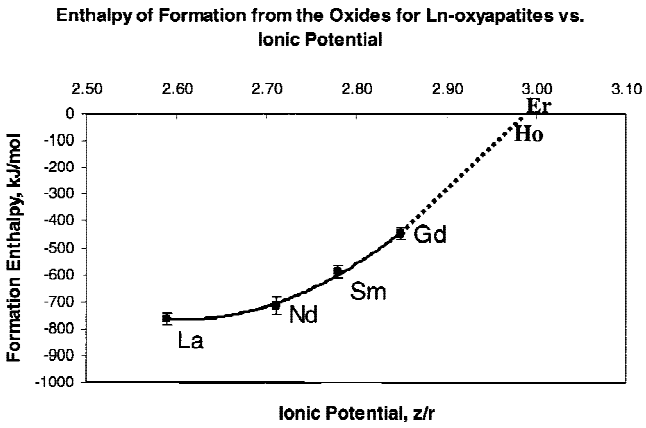

FIG. 1. The enthalpies of formation from the oxides for Ln oxyapatite phases plotted against the ionic potential of the Ln ion. The dotted line represents an extrapolation of the fitted data. Ln oxyapatite becomes metastable with respect to its oxides at Z/r = 2.98. The projected formation enthalpies for Ho Er oxyapatites indicate that Ho oxyapatite is barely stable with respect to its oxides whereas Er oxyapatite is metastable.

by a flattening of the enthalpy curve (Fig. 1). In a complex, multicomponent oxide, the bonding requirements of each cation–anion polyhedron must be satisfied if the structure is to remain stable with respect to other polymorphs or phase assemblages.[15] In the case of the Ln oxyapatites, substituting Sm for Gd stabilizes the structure by, presumably, better satisfying the bonding requirements of the Ln site in this complex silicate. This stabilization effect may continue until the Ln-site ion becomes too large and begins to destabilize the structure. The eventual destabilization of the structure is experimentally not attained, as there is no trivalent ion with ionic radius greater than lanthanum available. The importance of this observation is that it reveals a potential pit-fall with predictions of thermodynamic properties by extrapolating linearly beyond experimental data.[15] Future work will focus on the energetic trends of other Ln-bearing compounds such as the Ln oxycarbonates and Ln zirconate and titanate pyrochlores.

ACKNOWLEDGMENTS

This work was supported by the Center for High Pressure Research, a National Science Foundation Science and Technology Center. The microprobe analysis was performed at the Department of Geology at the University of California, Davis.

REFERENCES

1. K.P. Plucknett and D.S. Wilkinson, J. Mater. Res. **10,** 1387 (1995).
2. J. Lin and Q. Su, J. Alloys Compd. **210,** 159 (1994).
3. J. Lin, and Q. Su, Phys. Status Solidi (b), **196,** 261 (1996).
4. C.R. Ronda, T. Justel, and H. Nikol, J. Alloys Compd. **275–277,** 669 (1998).
5. A.N. Christiansen, R.G. Hazell, and A.W. Hewat, Acta Chem. Scand. **51,** 37 (1997).
6. F.K. Altenhein, W. Lutze, and R.C. Ewing, in *Scientific Basis for Radioactive Waste Management V*, edited by W. Lutze (Mater. Res. Soc. Symp. Proc. **2,** Pittsburgh, PA, 1982), p. 389.
7. L.M. Wang, M. Cameron, W.J. Weber, K.D. Crowley, and R.C. Ewing, in *Hydroxyapatite and Related Materials*, edited by P. Brown and B. Constantze (CRC Press, Boca Raton, FL, 1994), p. 243.
8. JCPDS card no. 09-0432.
9. J.I. Goldstein, D.E. Newbury, P. Echlin, D.C. Joy, A.D. Romig, Jr., C.E. Lyman, C. Fiori, and E. Lifshin, *Scanning Electron Microscopy and X-Ray Microanalysis*, 2nd ed. (Plenum Press, New York, 1992), p. 820.
10. A. Navrotsky, Phys. Chem. Miner. **24,** 222 (1997).
11. J.M. McHale, G.R. Kowach, A. Navrotsky, and F.J. DiSalvo, Eur. J. Chem. **2,** 1414 (1996).
12. A.J.G. Ellison and A. Navrotsky, J. Am. Ceram. Soc. **75,** 1430 (1992).
13. E. Takayama-Muromachi and A. Navrotsky, J. Solid State Chem. **106,** 349 (1993).
14. R.A. Robie, B.S. Hemingway, and J.R. Fisher, *Thermodynamic Properties of Minerals and Related substances at 298.15 K and 1 Bar (105 Pascals) Pressure and at Higher Temperatures* (U.S. Geol. Surv. Bull. 1452, Washington, D.C., 1979).
15. A. Navrotsky, Ceram. Trans. (2000, in press).